Journal of Magnetism and Magnetic Materials 324 (2012) 1011–1016

Contents lists available at SciVerse ScienceDirect

Journal of Magnetism and Magnetic Materials

journal homepage: www.elsevier.com/locate/jmmm

Numerical Renormalization Group computation of temperature dependent specific heat for a two-channel Anderson model

J.V.B. Ferreira [a,*], A.I.I. Ferreira [a], A.H. Leite [a], V.L. Líbero [b]

[a] Fundação Universidade Federal de Mato Grosso do Sul, Brazil
[b] Instituto de Física de São Carlos, SP, Universidade Estadual de São Paulo, Brazil

ARTICLE INFO

Article history:
Received 4 August 2011
Available online 15 October 2011

Keywords:
Multi-channel Anderson model
Local moment in compound and alloy
Kondo effect
Numerical Renormalization Group
Heavy fermion
Specific heat
Theories and models of many electron systems

ABSTRACT

The Numerical Renormalization Group (NRG) is applied to diagonalize a two-channel Anderson model describing a local magnetic impurity embedded in a fermionic bath. In spite of the difficulty in computing the specific heat using NRG, the *interleaving* discretization and *multi-step* iterative transformation virtually eliminate the numerical oscillations introduced by the logarithmic discretization of the conduction band. These allow to cover uniformly a large range of temperature, from the top of the band to a very small fraction of the bandwidth. This is relevant in describing, for instance, the presence of a low temperature Kondo resonance together with a high temperature Schottky peak, as well to cover Fermi and non-Fermi liquid regimes, like in the recent studied $Ce_{1-x}La_xNi_9Ge_4$ family. We highlight the importance in describing the Schottky peak to define the number of degrees of freedom of the local levels, in order to correctly define the model to describe a given compound.

1. Introduction

In order to observe Kondo and Schottky peaks in an experimental specific heat curve of a magnetic impurity embedded in a fermionic environment, like a metal, one must perform the measurements in a wide range of temperature. The Kondo peak, a resonance between a local spin and the conduction-electron spins, typically occurs at low temperatures, typically a few kelvins, while the Schottky peak, essentially due to the energy separation of the localized levels, usually occurs at much higher temperatures, $T \gtrsim 100$ K. On the theoretical side, to compute thermodynamical properties exhibiting both Kondo and Schottky peaks we face the challenge of a very large number of electronic states in the conduction band, which enormously difficult to the numerical diagonalization of the Hamiltonian. The Numerical Renormalization Group (NRG) [1,2] approach has been used with success in systems with local levels coupled to conduction states, due to its ability to treat different energy scale of the model Hamiltonian. Of particular interest is to compute specific heat versus temperature for multi-channel Anderson models, since they exhibit Fermi (FL) and non-Fermi liquid (nFL) regimes, often observed in real materials. However, specific heat being proportional to the difference $\langle (E-\langle E\rangle)^2/T^2\rangle$, at low temperature is numerically more difficult to obtain than, for instance, the magnetic susceptibility, which is just an average of the operator S_z^2. Our interest is to obtain the impurity contribution to the specific heat using the two-channel Anderson model (TCAM) [3,4], defined below, implementing the NRG with two improvements already introduced in the literature, the interleaving discretization [5,6] and the multi-step transformation [7]. These procedures allow to obtain any thermodynamical property in a wide range of temperature, covering from Kondo regime to Schottky peak, for both, FL or nFL regimes.

Usually the interest is in the low temperature regime, where the Kondo peak appears, and less attention is devoted to the Schottky peak, that appears at much higher temperature. Examples of both features in the same compound appears in Refs. [8,9], and also in Scheidt et al. [10], that uses a single Anderson impurity model with strong crystalline electric field, following the model proposed by Anders and Pruschke [11]. A standard NRG was used, and only the fit at low temperature was shown; the Schottky peak is not covered by their fit. Probably due to some feature of the NRG they used, their line of fit is not smooth. Although we do not claim a better fit to the experimental data using our single impurity model, our NRG results cover the temperature interval of both peak with a very smooth curve.

The use of the NRG approach has been intensified in recent years and a review about this technique was published in 2008 by Bulla and Costi [12]. One of the NRG basic concepts is the logarithmic discretization of the conduction band around the Fermi level. This procedure yields a large number of quantum states in the energy range corresponding to low temperatures. The undesirable consequence is the lack of representation of

* Corresponding author. Tel.: +55 67 3345 7034; fax: +55 67 3345 7450.
E-mail address: joao.ferreira@ufms.br (J.V.B. Ferreira).

0304-8853/$ - see front matter © 2011 Elsevier B.V. All rights reserved.
doi:10.1016/j.jmmm.2011.10.013

states near the top of the band, resulting in a low density of points for the specific heat curve at high temperatures, compromising the representation of the (usually sharp) Schottky peak. The discretization also introduces oscillations in every temperature dependent property, like specific heat. The NRG with interleaving discretization and multi-step transformation overcomes these limitations. We emphasize the importance of the high temperature regime of specific heat to better describe Schottky like peaks.

Next section presents the TCAM Hamiltonian which defines our model. In Section 3 we briefly describe our NRG procedure. In Sections 4 and 5 we present our data. In Conclusions we connect our theoretical work with experimental data of specific heat of a particular compound that exhibits some features of our model.

2. Two-channel Anderson model

The Kondo effect is one of the most important ingredient to explain several properties of real materials, as emphasized by Cox and Zwadowski in 1998 [13]. Experimental evidence about two-channel Kondo effect was reveled by Potok et al. [14]. Fig. 1 illustrates the TCAM we use in our analysis, first introduced in Refs. [3,4]. The metal is represented by an isotropic half-filled conduction band with bandwidth $2D$. The impurity is represented by a spin-doublet ground-state $|m,\sigma\rangle$ with m electrons and energy E_0. Through a channel [15] dependent hybridization V_α, $\alpha=1$ or 2, the impurity exchange one electron with the conduction band and may be leaved in one state of the two degenerate channel doublets $|m\pm1,\alpha=1,2\rangle$ with energy E_1.

The following Hamiltonian defines our model:

$$H = H_{bc} + H_{imp} + H_{hyb}, \tag{1}$$

$$H_{bc} = \sum_{k,\sigma,\alpha} \varepsilon_k c^\dagger_{\vec{k},\sigma,\alpha} c_{\vec{k},\sigma,\alpha}, \tag{2}$$

$$H_{imp} = E_1 \sum_\alpha |m-1,\alpha\rangle\langle m-1,\alpha| + E_1 \sum_\alpha |m+1,\alpha\rangle\langle m+1,\alpha| + E_0 \sum_\sigma |m,\sigma\rangle\langle m,\sigma|, \tag{3}$$

$$H_{hyb} = \sum_{k,\sigma,\alpha} V_\alpha (f^\dagger_{-1,\sigma,\alpha} c_{\vec{k},\sigma,\alpha} + h.c.), \tag{4}$$

where $f^\dagger_{-1,\sigma,\alpha} = |m,\sigma\rangle\langle m-1,-\alpha| + (2\sigma)|m+1,\alpha\rangle\langle m,-\sigma|$ (convention: $\alpha=-1\to\alpha=2$ and $\alpha=-2\to\alpha=1$)). The operators H_{bc}, H_{imp} and H_{hyb} represent the conduction band, the impurity and the impurity-band coupling respectively. $c^\dagger_{\vec{k},\sigma,\alpha}$ creates a free conduction electron with momentum $\vec{k}$, spin $\sigma=\pm1/2$, channel $\alpha=1$ or 2 and energy ε_k. The nFL behavior of this Hamiltonian comes from the interchanging of spin and channel degrees of freedom, thanks to the hybridization term H_{hyb}. This model is particle–hole symmetric, thus the Hamiltonian commutes with the isospin operators (or axial-charge) of each channel separately [3,4]. The square of the total spin is also conserved and commutes with isospin. Ref. [4] shows that for $V_1\neq V_2$ the magnetic susceptibility exhibits FL behavior, while for $V_1=V_2$ nFL behavior is obtained. Our data below for the specific heat also confirms these behavior. Appendix shows the equivalence of our model with a two-channel Kondo model, through the Schrieffer–Wolff transformation.

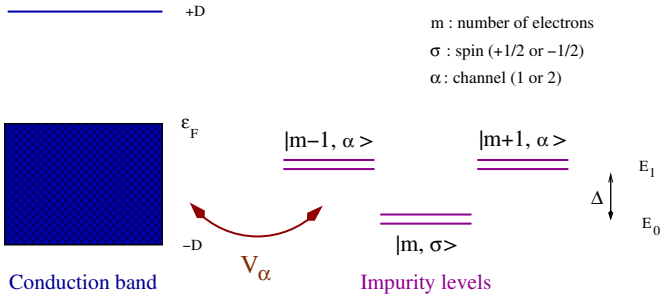

Fig. 1. Two-channel Anderson model (TCAM) diagram: the impurity levels hybridize with the conduction band states by two distinct channels, V_α, $\alpha=1$ or 2, receiving or losing an electron. The impurity is characterized by a spin-doublet ground-state ($\sigma=+1/2,-1/2$), with energy E_0, and two degenerate channel doublets ($\alpha=1,2$) with energy E_1. The conduction band extends from $-D$ to D, with the Fermi level $\varepsilon_F\equiv0$ in the middle.

3. The Numerical Renormalization Group

The NRG was first developed by Wilson [1] for the one-impurity one-channel Kondo problem and right after applied by Krishna-murthy et al. for the Anderson model [2]. Essentially, the NRG transforms the original Hamiltonian into a semi-infinite series of terms in decreasing order of energy scales; only the first term includes the coupling with the impurity. Each term is recursively built using the eigenstates of the previous term. This allows a truncation of states, based on relevant energy scales, with minor effects on impurity properties, rendering a non-perturbative numerical procedure from which we obtain the energy spectrum of the model.

As pointed out by Costi et al. [16], specific heat is a quantity more difficult to calculate than entropy or magnetic susceptibility. Thus, sometimes is preferable to obtain entropy and then numerically differentiate it with respect to temperature. However, this procedure itself introduces numerical errors, therefore in this work we compute specific heat directly using the NRG with interleaving discretization [5,6] and the two-step transformation [7] method instead. We briefly describe those methods below.

The use of NRG with interleaving method is very useful and is explained in detail in Refs. [5,6]. Here we just summarize some ideas about its application to obtain specific heat curves. The NRG procedure starts with the logarithmic discretization of the conduction band, replacing its continuum by a set of discrete energy states defined in the interval $\Lambda^{-n-1}\leq|\varepsilon_n|\leq\Lambda^{-n}$, for all integer n and $\Lambda>1$. As a consequence, all thermodynamical properties plotted as a function of the temperature shows oscillations reflecting the discretization of the conduction band, with very large amplitudes in the particular case of the specific heat.

To smooth these artificial oscillations, the interleaving method prescribes to execute the NRG procedure with two discretization parameters. The discrete energy states are now defined in the interval $\Lambda^{-n-1-z}\leq|\varepsilon_n|\leq\Lambda^{-n-z}$, with $z>0$. With fixed Λ, we compute the physical property of interest averaging it over an unitary interval of z. We linearly discretize this unitary interval and for magnetic susceptibility or entropy an average with only two values of z differing by 1/2 is enough to virtually eliminate the oscillations. For specific heat, however, a few more z are necessary to eliminate the oscillations. The advantage is, the processing time is almost linear in z, but goes roughly as $\exp(1/\ln\Lambda)$, so in order to recover the continuum of the conduction band is preferable to maintain a fixed Λ and work with several z than to decrease Λ close to unity. It is easy to see that, using a given Λ and two values of z differing by 0.5 renders almost equivalent curves if implemented with the usual NRG (that is, $z=1$) but using the square root of Λ; the last case, however, takes a much higher processing time and uses much more memory space. Fig. 2 gives an idea of how large are the oscillations without the interleaving and the efficiency of this smoothing procedure.

The usual logarithmic discretization of the conduction band around the Fermi level naturally enhances the low temperature

energy scales, but introduces few energy states in the high temperature interval. Because of this, Schottky peak is poorly described using only one discretization parameter. The interleaving, in addition, increases the number of points in all temperature interval simply working with several values of z.

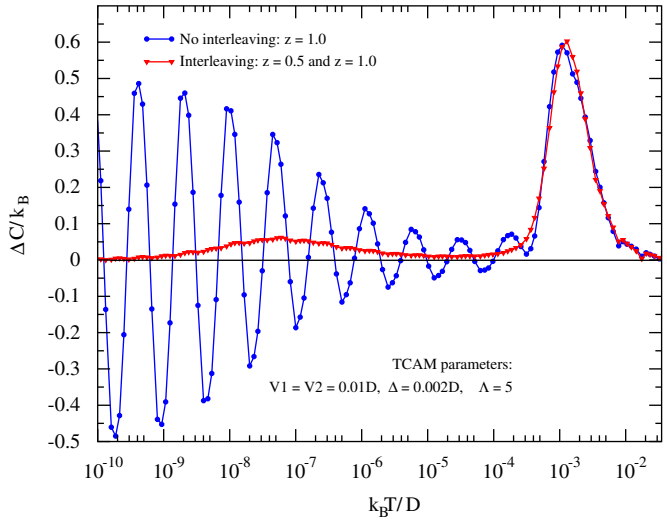

Fig. 2. Temperature dependent specific heat curves obtained from the usual NRG implementation with only one discretization parameter ($z=1$) showing the huge oscillations due to the discretization of the conduction band. The interleaving with two z, 0.5 and 1, practically removed the oscillations. Note the large value of Λ used. To obtain that smooth curve using only $z=1$ would be necessary to work with $\Lambda \approx 2$ ($\approx \sqrt{5}$), demanding much more processing time and memory space. The symmetric case $V_1 = V_2$ introduces a large number of degenerate eigenstates of the Hamiltonian, which causes an increase of the oscillating amplitude relative to the cases $V_1 \neq V_2$. Also note the larger number of points used to build the smoothed curve, thanks to the interleaving process.

The multi-step transformation method in NRG is described in detail in Ref. [7]. Here we just summarize the main ideas. For the TCAM, the size of the basis state from one NRG iteration to the next grows by a factor 16, corresponding to create one electron with spin up, or down, or two electrons, or none, in both channels; this is four times the growing rate of the one-channel model. Besides more time consuming, this rapidly reaches the limit of computer memory as the NRG iterations advance. The idea is to separate each NRG iteration in two steps: in the first, we grow the basis states corresponding to channel one, and in the second step we complete the basis states growing them with the operators of the channel two. Thus, in each step, the basis grows by a factor four. An energy cutoff is used in each step separately, and that saves time and memory by excluding high energy state in every step, before they can propagate to the next iteration. Ref. [7] comments the reduction of computational memory and time processing when multi-step transformation is used in the calculation of the magnetic susceptibility of the TCAM, in both FL ($V_1 = V_2$) and nFL ($V_1 \neq V_2$) regimes.

4. Specific heat for the TCAM

Fig. 3 shows our curves for the impurity specific heat and entropy as a function of temperature for several parameters of our TCAM, obtained using the interleaving and the two-step transformation. The specific heat data are obtained from the definition

$$C(T)/k_B = \frac{\langle E^2 \rangle - \langle E \rangle^2}{(k_B T)^2}, \tag{5}$$

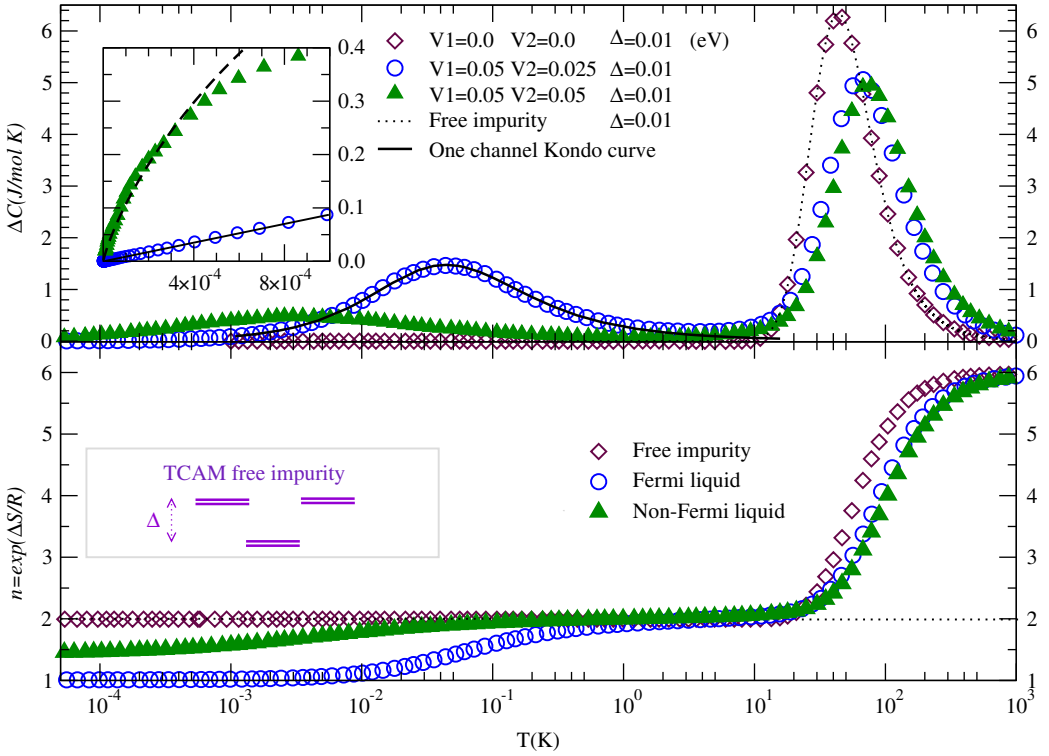

Fig. 3. Impurity contribution to the specific heat, ΔC, and the exponential of the entropy $n = \exp(\Delta S/R)$, as a function of temperature for our TCAM ($R = k_B \cdot N_A$). The ($\diamond$) are data for an isolated impurity with energy-level separation $\Delta = 0.01$ eV, showing only the Schottky peak. For $V_1 \neq V_2 \neq 0$ the Kondo peak appears besides the Schottky one ($\circ$). The continuous line is a fit using the universal Kondo specific heat curve for $T_k = 0.07$ K. The corresponding curve in the inset shows a linear behavior of ΔC, characteristic of a FL regime. The Kondo singlet formed in this case implies $n=1$ as shown in the lower plot ($\circ$). For $V_1 = V_2$ we have the nFL regime ($\blacktriangle$), the specific heat curve at low temperature follows the $-T/T_k \ln T/T_k$ dependence, with $T_k = 0.0093$ K in this case. The number of effective degrees of freedom, n, at very low temperature reaches the value 1.44731, very close to $\sqrt{2}$, as a consequence of the overscreened local spin. For all curves we have $n=6$ at high temperature, reflecting the almost degenerate states of the impurity in this limit ($k_B T \gg \Delta$). For the interleaving we used 16 values of z, with $\Lambda = 5$.

where $\langle O \rangle$ means thermodynamical average over the physical property O. The entropy is calculated from

$$S(T)-S(0) = \int_0^T C(T')\, d\ln(T'), \tag{6}$$

that is, through the area below the specific heat curve. We could also compute the entropy directly via $S(T) = \ln Z(T) + \langle E \rangle / k_B T$, where $Z(T)$ is the partition function, resulting practically in the same curve. This is so due to the smoothness of the specific heat curve thanks to the interleaving. In all figures, we plot the impurity contribution to the physical property, that is, we always subtract the contribution from the free conduction band. As a reference, we plot in Fig. 3 the trivial case of $V_1 = V_2 = 0$, representing an isolated impurity. The dotted line is the analytical curve for this case and the ($\diamond$) our data. There is no Kondo resonance in this case, only the Schottky peak since we just have a decoupled two-level system. The exponential of the (impurity) entropy, $n = \exp(\Delta S/k_B)$, which measures the effective degrees of freedom of the impurity, in this case ($\diamond$) starts at 6 for high temperature, $k_B T \gg \Delta$, since all six levels of the impurity are practically degenerated, and drops to 2 at much lower temperature where the two-channel doublets are inaccessible, resting only the spin doublet as the impurity ground state. The open circles ($\circ$) depict the case of $V_1 = 0.05 \neq V_2 = 0.025$. Besides the Schottky peak, now the hybridization with the conduction band generates the Kondo peak. The continuous line among these data is the Kondo universal curve obtained from Bethe ansatz, using the Kondo temperature $T_k = 0.07$ K, for the Fermi liquid regime of the one-channel Kondo model. For this case, the impurity entropy starts at $\ln 6$ at high temperature, drops to $\ln 2$ when the temperature is in the interval $k_B T_k < k_B T < \Delta$. This is the formation of a local moment with the flipping of the two components of the spin doublet. At lower temperature, the conduction electrons and the spin doublet form the Kondo singlet state, and as a consequence, the exponential of the impurity entropy reaches the unit. More interesting is the case of $V_1 = V_2$, (▲). The Schottky peak and the local moment regime are similar to the case $V_1 \neq V_2$, but the two-channel hybridizations with the conduction band overscreened the impurity and the ground state now shows more than one but less than two effective degrees of freedom, which can be seen in the value of the exponential of the impurity entropy that goes to $\sqrt{2}$ [15]. This is the two-channel Kondo resonance, a peak more than four decades of temperature below the Schottky one. Another feature of these plots is that the Schottky peak for the isolated impurity ($\diamond$) is higher than any other, that is, the coupling with conduction electrons tends to weaken this peak.

5. Practical evaluation of the Kondo temperature

Fig. 4 shows plots of temperature times magnetic susceptibility, in units of $(g\mu_B)^2$, versus the temperature T scaled by T_k. For the cases with $V_1 \neq V_2$, the T_k is determined using the universal Kondo susceptibility (continuous line in Fig. 4), since this case represents a FL regime. For the curves with $V_1 = V_2$, showing nFL behavior, we find T_k from the best fit at low temperature through the formula

$$T\chi \approx -0.103 \frac{T}{T_k} \ln \frac{T}{T_k}, \tag{7}$$

expected to be valid for a two-channel model in this temperature interval [15]. The prefactor 0.103 is empirical. We note from Fig. 4 that all curves, exhibiting Fermi or non-Fermi liquid behavior, have the property that $k_B T_k \chi(T_k)/(g\mu_B)^2$ equals to 0.0701 [2]. This has been used in the on-channel models to find T_k, since the magnetic susceptibility is easy to obtain due to its low amplitude of oscillations. We note from this figure that this procedure estimates T_k for the two-channel model as well.

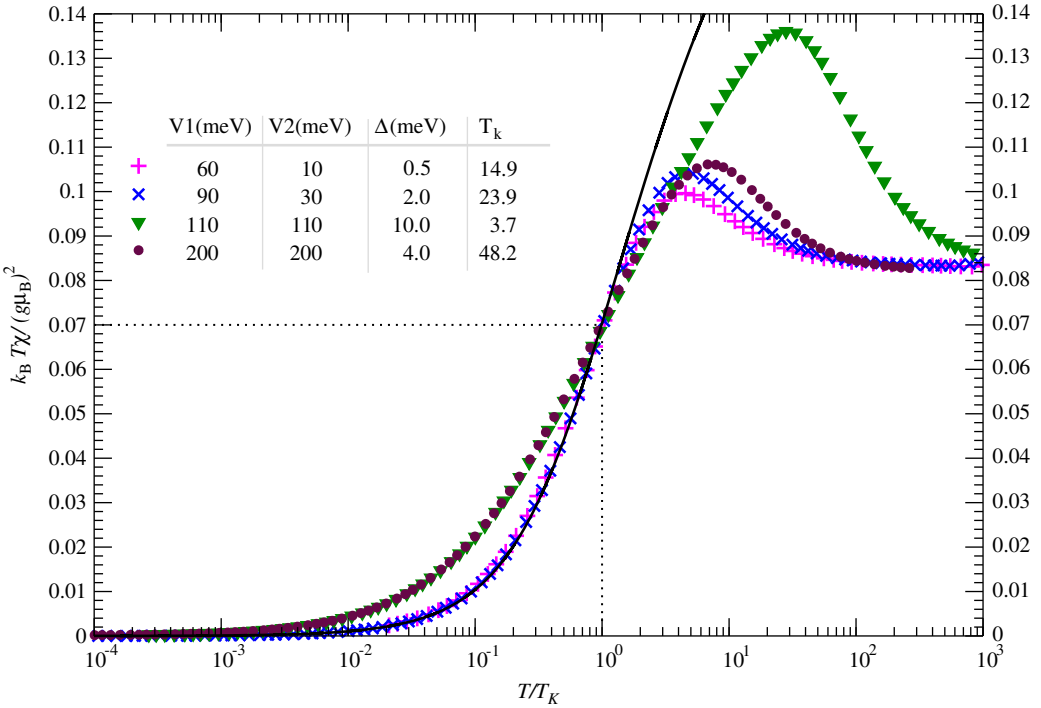

Fig. 4. Impurity magnetic susceptibility in units of $(g\mu_b)^2$, versus temperature scaled by T_k. At T_k, all curves yields $k_B T_k \chi/(g\mu_b)^2 \approx 0.0701$. We may use this property to estimate T_k. The continuous line is the universal Kondo susceptibility, that fits the low temperature interval for all cases with $V_1 \neq V_2$. All curves reach the value 1/12 at very high temperature, consistent with two magnetic levels (the spin doublet) among six practically degenerate levels for $k_B T \gg \Delta$). For the interleaving we used four values of z, with $\Lambda = 5$.

6. Conclusions

The model defined by the Hamiltonian (1) exhibits FL and nFL regimes, as shown in the specific heat curves above. Our NRG procedure is able to cover a large temperature interval, from a Kondo resonance to a Schottky peak. The interleaving and the multi-step procedures make it possible to work with large discretization parameter Λ, without the inconvenience of large oscillations. This reduces time processing and memory space, in this way allowing to treat more realistic models. Our theoretical approach may be relevant in the study of compounds like $Ce_{1-x}La_xNi_9Ge_4$, which show, for special stoichiometry, huge Sommerfeld coefficient $\gamma = \Delta C/T \approx 5.5\ \mathrm{J\,K^{-2}\,mol^{-1}}$ [17], FL and nFL regimes. In particular, Scheidt et al. published the experimental electronic specific heat curve for the case $x=0.5$ [10, Fig. 2a], and interpreted the data as a Kondo peak separated by more than two decades of temperature from a Schottky peak. In spite of the high concentration of Ce, in order to analyze the data [17], Scheidt et al. used a single-impurity Anderson model with strong crystalline electric field. They diagonalized their model using standard NRG, but showed only the fit at low temperature; they claim the Schottky peak is absent in their NRG fits.

An attempt to fit the experimental data for $Ce_{0.5}La_{0.5}Ni_9Ge_4$ shows lack of local degrees of freedom in our model to describe the Schottky peak. The experimental value of the specific heat Schottky peak is about 8 J/mol K, while our peak for the free impurity case reaches only 6 J/mol K. The hybridization, needed to obtain the Kondo peak, will reduce this value (this tendency can be seen in Fig. 3) increasing even more the discrepancy. This indicates that the model for this compound should have a more complex structure in the local levels. Apparently, the shape of the Schottky-like peak in this compound suggests a $J=9/2$ multiplet at the impurity level (the origin could be the ionized state Ce^{+1} in the compound). A more careful analysis of this compound should be done since it is possible that what Ref. [10] claims to be a Kondo peak (at about $T=5$ K) is in fact a second Schottky peak (the first one is at $T \approx 50$ K) due to more complex local structure of levels, with the Kondo peak merged in the tail of this peak at much lower temperature. We say that based on the small intensity normally obtained from a Kondo peak, typically less than 0.5 J/mol K in the nFL regime (see Fig. 3).

We did not attempt a fine tuning of parameters, since our model still need to be improved in order to describe such complex compounds, but we just want to sign that our model has the main features and the NRG indeed is capable to yield both Kondo and Schottky peaks even in situations with nFL behavior. We believe in the potential use of NRG with large discretization parameter Λ, together with interleaving and multi-step transformation, opening the way to numerically deal with more realistic models, as it seems to be required by some relevant compounds. We are addressing our research in this direction, improving our model, mainly in the impurity local levels.

Acknowledgment

We thank the support of the Brazilian agencies CNPq, CAPES and FUNDECT-MS.

Appendix

Although the results of Ref. [4] for the magnetic susceptibility, and the present data for the specific heat, are typical of a two-channel model, mainly because the presence of the nFL regimes, we prove here the equivalence of our model with the two-channel Kondo model at low excitation energies, by performing a Schrieffer–Wolff transformation [18,19]. To do that, we first rewrite the Hamiltonian, Eq. (1), as $H = H_0 + H_{hyb}$, where H_{hyb} given as before and

$$H_0 = \sum_{k,\sigma,\alpha} \varepsilon_k c^\dagger_{\vec{k},\sigma,\alpha} c_{\vec{k},\sigma,\alpha} + \sum_{\alpha,i} E_{|i|}\, |m+i,\alpha\rangle\langle m+i,\alpha|, \tag{8}$$

where $i=-1,0$ or 1. In the Kondo physics, one local spin flips between its states $\sigma = \pm 1/2$. In our model this is a process in second order in V_α, therefore, we look for an equivalent Hamiltonian $\tilde{H} = e^P H e^{-P}$ that does not contain linear terms in V_α, that is, in the expansion

$$\tilde{H} \approx H_0 + H_{hyb} + [P,H_0] + [P,H_{hyb}] + \mathcal{O}(V_\alpha^3) \tag{9}$$

we look for P, at least linear in V_α, such that

$$[P,H_0] = -H_{hyb}, \tag{10}$$

and therefore up order V_α^2,

$$\tilde{H} \approx H_0 + [P,H_{hyb}]. \tag{11}$$

For two eigenstates $|a\rangle$ and $|b\rangle$ of H_0, with energies E_a and E_b, Eq. (10) implies that $\langle a|P|b\rangle = \langle a|H_{hyb}|b\rangle/(E_a - E_b)$. Multiplying this relation at right by $|a\rangle$ and at left by $\langle b|$ we find

$$P = \sum_{a \neq b} \frac{\langle a|H_{hyb}|b\rangle}{E_a - E_b} |a\rangle\langle b|. \tag{12}$$

The term H_{hyb} connects states that exchange one particle between impurity and conduction band: $|m,\sigma\rangle \to |m-1,\alpha\rangle$, with energy $\varepsilon_k + E_1 - E_0$, or $|m+1,\alpha\rangle \to |m,\sigma\rangle$, with energy $\varepsilon_k + E_0 - E_1$, and Hermitian conjugates. Collecting all possible states of this kind, we build the operator P as

$$P = \sum_{\vec{k},\sigma,\alpha} V_\alpha \left[\left(\frac{|m-1,-\alpha\rangle\langle m,\sigma|}{\varepsilon_k + E_1 - E_0} + (2\sigma) \frac{|m,-\sigma\rangle\langle m+1,\alpha|}{\varepsilon_k + E_0 - E_1} \right) c_{\vec{k},\sigma,\alpha} - h.c. \right]. \tag{13}$$

This operator obeys the condition (10) for excitations near de Fermil level ($\varepsilon_k \approx 0$, or $k \approx k_F$). In this way,

$$[P,H_{hyb}] = \sum_\alpha J_\alpha \vec{s}_\alpha \cdot \vec{S}, \tag{14}$$

where

$$\vec{S} = \sum_{\mu,\nu} \left\langle m,\mu \left| \frac{\vec{\sigma}_{\mu,\nu}}{2} \right| m,\nu \right\rangle,$$

$$\vec{s}_\alpha = \sum_{\vec{k},\vec{q},\mu,\nu} c^\dagger_{\vec{k},\mu,\alpha} \frac{\vec{\sigma}_{\mu,\nu}}{2} c_{\vec{q},\nu,\alpha},$$

$$J_\alpha = \frac{8V_\alpha^2}{E_1 - E_0}, \tag{15}$$

with $\vec{\sigma}$ the Pauli matrices. Finally, from (11) we obtain

$$\tilde{H} \approx H_0 + \sum_{\alpha=1,2} J_\alpha \vec{s}_\alpha \cdot \vec{S}, \tag{16}$$

which is the two-channel Kondo Hamiltonian for a local spin $\vec{S}$. The sign of $\Delta \equiv E_1 - E_0$ decides between ferro- or anti-ferromagnetic ordering.

References

[1] K.G. Wilson, Reviews of Modern Physics 47 (1975) 773.
[2] H.R. Krishna-murthy, J.W. Wilkins, K.G. Wilson, Physical Review B 21 (1980) 1003–1043.
[3] J.V.B. Ferreira, L.N. Oliveira, D.L. Cox, V.L. Líbero, Journal of Magnetism and Magnetic Materials 226–230 (2001) 196–198.
[4] J.V.B. Ferreira, L.N. Oliveira, D.L. Cox, V.L. Líbero, Journal of Magnetism and Magnetic Materials 226–230 (2001) 132–133.

[5] W.C. Oliveira, L.N. Oliveira, Physical Review B 49 (1994) 11986–11994.
[6] S.C. Costa, C.A. Paula, V.L. Líbero, L.N. Oliveira, Physical Review B 55 (1997) 30.
[7] J.V. Ferreira, V.L. Líbero, L.N. Oliveira, Computer Physics Communications 174 (2006) 862–868.
[8] L. Peyker, C. Gold, E.-W. Scheidt, W. Scherer, J.G. Donath, P. Gegenwart, F. Mayr, T. Unruh, V. Eyert, E. Bauer, H. Michor, Journal of Physics: Condensed Matter 21 (2009) 235604.
[9] M. Falkowski, A. Kowalczyk, T. Tolinski, Journal of Alloys and Compounds 509 (2011) 6135–6138.
[10] E.W. Scheidt, F. Mayr, U. Killer, W. Scherer, H. Michor, E. Bauer, S. Kehrein, T. Prushke, F. Anders, Physica B: Condensed Matter 378–380 (2006) 154–156.
[11] F.B. Anders, T. Pruschke, Physical Reviews Letters 96 (2006) 086404.
[12] T.P.R. Bulla, T.A. Costi, Reviews of Modern Physics 80 (2008) 395.
[13] A. Cox, D.L. Zawadowski, Advances in Physics 47 (1998) 599–942.
[14] R. Potok, I. Rau, H. Shtrikman, Y. Oreg, D. Goldhaber-Gordon, Nature 446 (2007) 167–171.
[15] P. Nozieres, A. Blandin, Journal of Physics 41 (1980) 193.
[16] T.A. Costi, A.C. Hewson, V. Zlatic, Journal of Physics: Condensed Matter 6 (1994) 2519–2558.
[17] U. Killer, E.W. Scheidt, G. Eickerling, H. Michor, J. Sereni, T. Pruschke, S. Kehrein, Physical Review Letters 93 (2004) 216404.
[18] J.R. Schrieffer, P.A. Wolff, Physical Review 149 (1966) 491.
[19] S. Kehrein, A. Mielke, Annals of Physics 252 (1996) 1–32.